ICAS 2021 SHANGHAI
International Council of the Aeronautical Sciences
32nd Congress of the International Council of the Aeronautical Sciences
September 6-10, 2021
Pudong Shangri-La, Shanghai, China

Research On Airborne RF System Testing Technology Using TDR Technique

Wenjing Mo 1, Xiaoxuan Huang 1, Jianan Cao 2, Qi Yin 1 & Xiaohua Wu 1

1 Chengdu Aircraft Industrial (Group) Co. Ltd, Chengdu 610092,China
2 School of Electrical Engineering, Xi'an Jiaotong University, Xi'an 710049,China

Abstract

In this paper, by constructing network models of the airborne radio frequency system, a signal suitable for transmission in the aircraft radio frequency network is studied, and the time domain reflection-based radio frequency system network performance test simulation and influencing factor analysis are performed, and a method suitable for aircraft radio frequency network testing Carry out application verification, fault diagnosis and effect evaluation of the airborne radio frequency system network.

Keywords: Aviation cable, TDR, Gaussian wave, Fault Location

1. General Introduction

As the "nervous system" of the aircraft, airborne cables are responsible for tasks such as electrical connection and signal transmission. Ensuring their integrity and reliability has always been a very important part of aircraft production and maintenance. During the use of the aircraft, the cables may cause insulation failure, open circuit failure or short circuit between wires due to wear, corrosion, aging, etc., resulting in interruption of signal transmission, and in severe cases, arcing may even damage neighboring cables and equipment[1] , Causing a fire, causing a major aircraft accident. Therefore, in order to ensure safety, the airborne cables need to be maintained and overhauled regularly.

The detection of cable faults requires specific test methods. For cable disconnection or short-circuit faults, the more widely used method in the industry is the time domain reflectometry [2].

Time domain reflectometry (TDR) is based on the phenomenon that when electromagnetic waves propagate on the transmission line, the impedance mismatch points, such as short-circuit points, short-circuit points, intermediate joints, etc., reflect and generate echoes. It is used in the field of cable length measurement, fault location, etc. A widely used method that is easy to implement, lossless, fast, and high in accuracy in practical applications [3]. It injects low-voltage pulses into the guide wire, analyzes the characteristics of the reflected signal to determine the type of fault, measures the time difference between the incident wave and the reflected wave of the fault, and determines the location of the fault. This technology has always been the focus of attention of experts and scholars in the field of testing. There are researches on various fault models of coaxial cables [4], the evaluation of cable characteristic impedance based on time-domain reflection waveforms [5], and new TDR pulse generation Circuit design [6], there are various directions to study the key part of the measurement error in the TDR technology [7].

At present, the application of TDR technology in foreign countries to manufacture test instruments has been relatively mature. For example, the British Radiodetection T625 advanced cable tester has pulse width adjustment and large-screen display functions, high precision and good dynamic response. Seba T30E wave reflection method cable fault locator is suitable for low resistance and disconnection fault location of 220kV~330kV power cables. Domestic cable testing products are mainly used in fields such as communications and electric power, and the overall resolution is low. For example, the HT-TC cable fault tester produced by Huatian Power can detect cable short-circuit, disconnection, poor contact and other faults with an accuracy of 1m. The ST-500E cable fault tester produced by Xidian Machinery Electronic Instrument Factory can measure cable length

and The speed of electromagnetic waves propagating in the cable, but there is a measurement blind zone of 15m [8].

In summary, the current foreign cable fault detection technology is relatively mature, and the detection efficiency of cable short-circuit and open-circuit faults is relatively high, but it is expensive and not suitable for large-scale promotion. However, the domestic cable fault detection technology, especially for aviation cable detection technology, is relatively backward. The design resolution needs to be improved, and there is a blind zone when the cable is short [9], and there is room for improvement.

By consulting the product information, it is found that the existing cable fault detectors using TDR technology mostly choose rectangular pulses or step pulses in the selection of transmitted pulses, but the steep pulse edges contain more high-frequency components, and the echo will be attenuated due to each frequency component. The inconsistency will produce distortion, which will not be conducive to the judgment of the reflection point, and will cause deviations in the measurement results [10]. This paper uses Gaussian waves with gentle rising and falling edges. Both peaks and valleys are easier to identify [11]. At the same time, according to the characteristic that Gaussian pulses are still Gaussian waves after attenuation in the frequency domain, the originality is The spectrum attenuation degree is used to calculate the cut-off frequency of the cable, which realizes the measurement of the transmission bandwidth, and provides a multi-faceted reference for the user.

In this paper, a fault model of aeronautical cables is established, and a series of simulations and related experiments with Gaussian waves as incident waves are carried out. The results show that this method has a good effect on the fault judgment and fault location of airborne cables.

2. The principle of fault location test based on TDR technology

2.1 TDR technology principle

The time-domain reflection method TDR is used to realize cable measurement (take open circuit fault as an example), and its basic principle is shown in Figure 1 [12]. Suppose the length of the cable to be tested is ΔL, an electric pulse is sent out at t_1, and the timing signal START is started; since the end of the cable is in an open state, when the electric pulse reaches the end, a reflected wave is formed, and then it is transmitted back to form a transmission pulse. The reflection time is recorded as t_2, and a stop timing signal STOP is issued; by calculating the time difference Δt between t_2 and t_1, the cable length ΔL can be obtained.

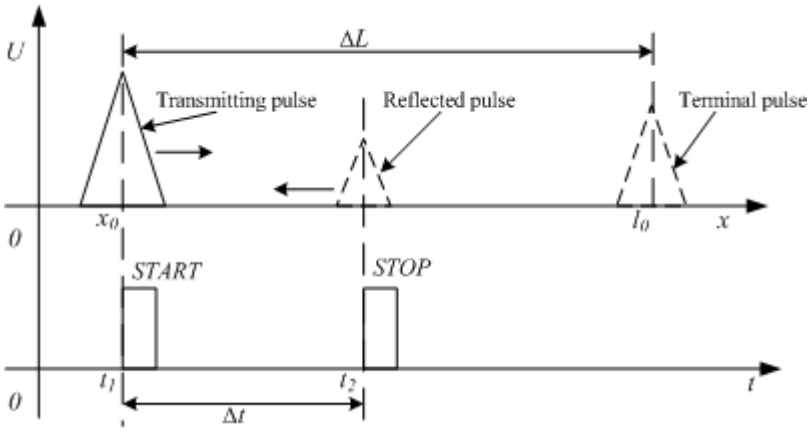

Figure 1 – Schematic diagram of TDR fault location principle.

The mathematical expression is

$$D_L = \frac{1}{2}\frac{C}{\sqrt{e_r}} \times D_t \quad (1)$$

In the formula (1) , c is the speed of light, and ε_r is the relative permittivity of the cable. This value is only related to the insulating material of the cable, generally between 1.5 and 3. It can be seen from this formula that determining the wave velocity of the pulse in the cable is very important for accurately calculating the distance to the fault [13]. When the wave velocity value of the cable is

not clear, the following method can be used to measure: use a cable made of the same material with a known length, and according to the time between capturing the transmitted pulse and the reflected pulse at the cable end, the cable can be calculated The wave velocity is

$$v = \frac{2l}{D_t} \tag{2}$$

Then substitute the wave velocity obtained from the above formula into the formula (1) for general measurement. According to the time difference between the captured START signal and the STOP signal, the distance between the fault point and the test point can be obtained. For example, if there is a waveform as shown in Figure 2, when the wave speed is unknown and the length is known, the interval D_t between the two peaks is used to calculate the wave speed; when the wave speed is known but the length is unknown, D_t is used to calculate the length.

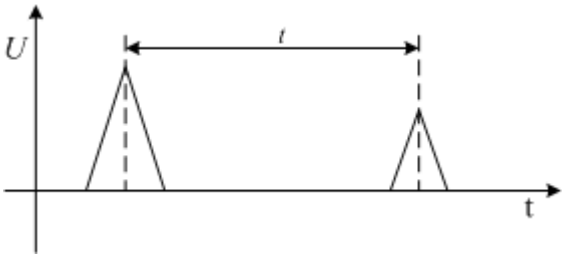

Figure 2 –Schematic diagram of incident wave and echo.

In addition, the echo changes from an obvious peak to an obvious trough during a short-circuit fault, and there will be a superposition of multiple peaks and troughs in the case of cable bifurcation or low-resistance faults, which need to be distinguished according to the specific situation [14].

2.2 The characteristics of Gaussian waves and the theoretical basis of bandwidth testing

The waveform of the Gaussian wave is like a Gaussian function, and its mathematical expression is

$$f(x) = \frac{A}{\sqrt{2\pi}\cdot\sigma} e^{-\frac{(x-x_0)^2}{2\sigma^2}} \tag{3}$$

Ideally, the Fourier transform results are as follows:

$$F(\omega) = A \cdot e^{-\frac{1}{2}\sigma^2 \cdot \omega^2} \tag{4}$$

As shown in Figure 3, the spectrum waveform is still Gaussian, containing relatively few high-frequency components.

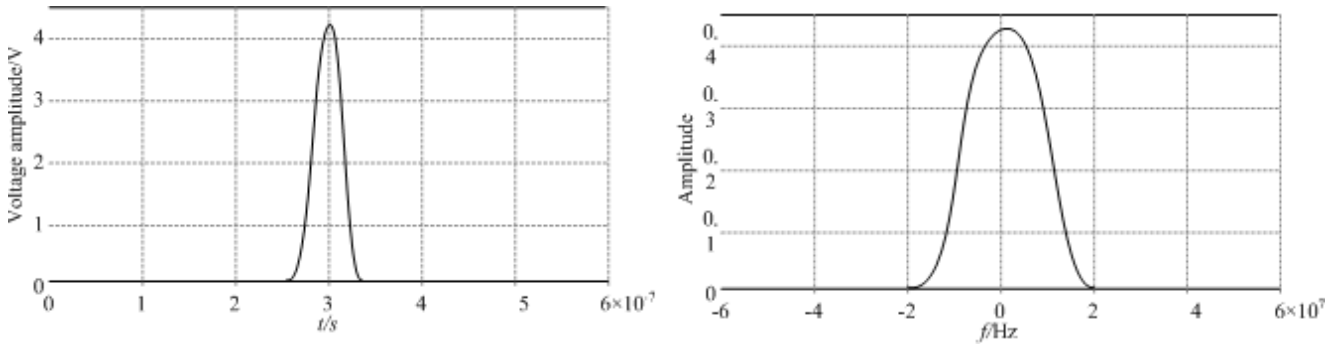

Figure 3 –Time-domain waveform and spectrogram of Gaussian wave.

According to the electromagnetic field theory, the wire itself has inductance, and the capacitance between the wire and the wire and between the wire and the ground is called stray capacitance or distributed capacitance. The capacitance and inductance will block the signal and consume the signal energy, if it is serious, it will affect the signal [15]. This effect is directly proportional to the frequency of the alternating current signal. When the frequency is high to a certain level, it is difficult for the signal to remain stable, and the entire circuit will naturally not work properly. For this reason, the concept of "bandwidth" is proposed in electronics, which refers to the frequency range in which the circuit can maintain stable operation.

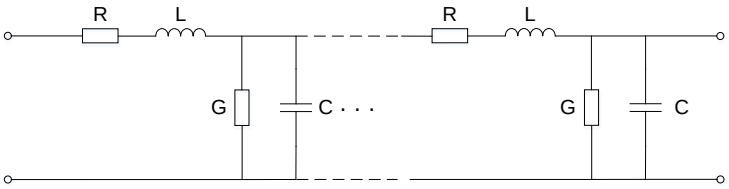

Figure 4 –Transmission line equivalent model.

According to transmission line theory and equations, the transmission of electrical pulse signals through a distance of $\Delta L = x\text{-}x_0$ causes its amplitude to attenuate, and its attenuation function is

$$H(\omega, x) = e^{-\alpha(\omega)(x-x_0)-j\beta(\omega)(x-x_0)} \tag{5}$$

In the formula, α is the transmission attenuation coefficient, in dB/m; β is the transmission phase shift constant, in *rad/m*. According to the transmission line equivalent model in Figure 4 [16],their calculation expressions are

$$\alpha = \frac{\sqrt{2}}{2}\sqrt{(R_0G_0 - \omega^2 L_0C_0) + \sqrt{(R_0^2 + \omega^2 L_0^2)(G_0^2 + \omega^2 C_0^2)}} \tag{6}$$

$$\beta = \frac{\sqrt{2}}{2}\sqrt{(\omega^2 L_0C_0 - R_0G_0) + \sqrt{(R_0^2 + \omega^2 L_0^2)(R_0^2 + \omega^2 C_0^2)}} \tag{7}$$

Under the condition that the reflection coefficient is l_0, and the cable length is L, the reflected wave is expressed as

$$f(x) = \frac{A}{\sqrt{2\pi}\cdot\sigma} e^{-\frac{(2l_0+x_0-x)^2}{2\sigma^2} - [\alpha(\omega)+j\beta(\omega)](2l_0+x_0-x)} \tag{8}$$

As the cable length increases, due to the phenomenon of attenuation and dispersion, the attenuation of the Gaussian wave high-frequency components is more serious for the lower frequency components. It is reflected in the formula that the attenuation constant α will increase with the increase of the angular frequency, so The reflected waveform no longer fully satisfies the Gaussian wave characteristics, resulting in a reduction in the ideal bandwidth. The reflected time-domain waveform is shifted to the same reference as the transmitted time-domain waveform as shown in Figure 5.

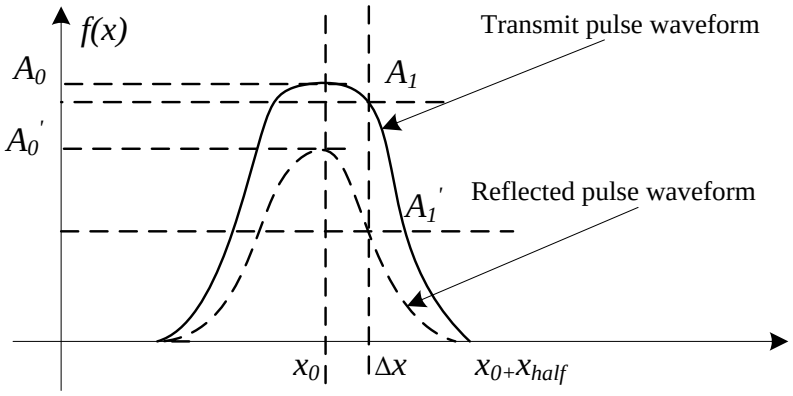

Figure 5 –Comparison of Gaussian wave transmitted waveform and reflected waveform.

Through spectrum analysis, we can get

$$F(\omega) = A \cdot e^{-\frac{1}{2}\delta^2\cdot\omega^2 - \alpha(2l_0+x_0-x)} \tag{9}$$

Obviously, when both the maximum amplitude point and the center of the spectrum appear at $x=x_0$,For ease of presentation, set

$$l = 2l_0 + x_0 - x \tag{10}$$

Under high frequency conditions, the attenuation constant α is proportional to the angular frequency $\alpha=k\cdot\omega$, so after the waveform has passed the length l, consider the attenuation -3dB condition

$$e^{-\frac{1}{2}\sigma^2\cdot\omega^2-k\omega l}=\frac{\sqrt{2}}{2} \tag{11}$$

So the expression for the attenuation -3dB bandwidth is

$$BW(l)=\frac{-kl+\sqrt{k^2l^2+\sigma^2 ln\,(2)}}{2\pi\sigma^2} \tag{12}$$

According to experience, if k=1.273×10^{-9} [17], because the relationship between the half pulse width x_{half} and σ of the Gaussian wave is

$$x_{haif}=\sqrt{2ln\sqrt{2}} \tag{13}$$

According to equations (12) and (13), the -3dB bandwidth changes of pulses propagating in different cable lengths are shown in Figure 6.

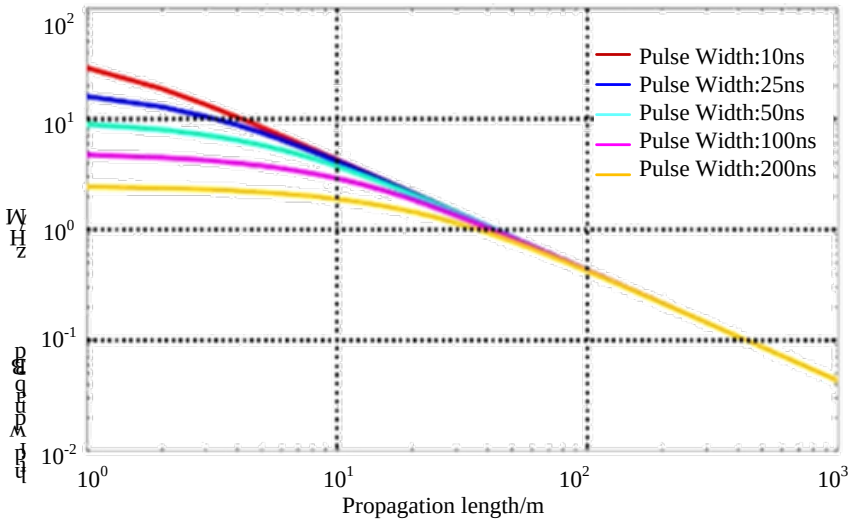

Figure 6 –Variation of -3dB bandwidth of Gaussian wave with different pulse width with propagation length.

It can be seen from the figure that the higher the signal frequency, the faster the signal bandwidth attenuates as the propagation length increases. At the same time, it can be known that when the cable length reaches 100m, the bandwidth drops below 1MHz; when the length is 1km, the bandwidth drops below 100kHz.

3. Modeling and simulation

In order to verify the rationality of the design, the following model is established using the Simulink simulation platform, and the relevant parameters are set.

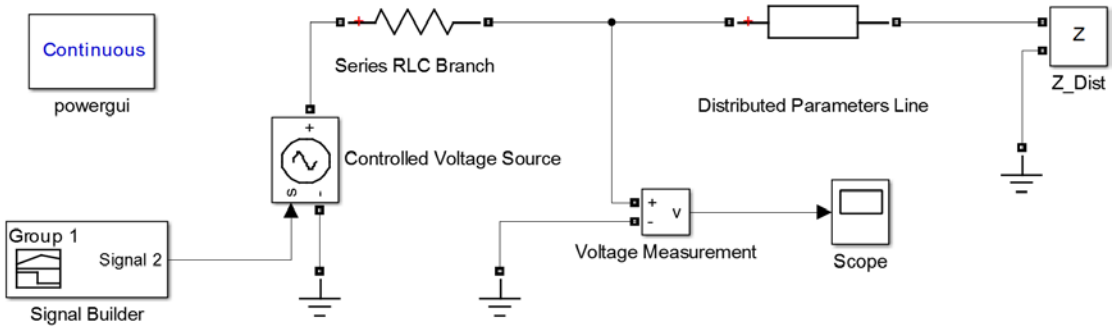

Figure 7 – Simulink simulation circuit diagram.

According to the Simulink simulation circuit shown in Figure 7, the waveforms collected at the initial end of the cable are:

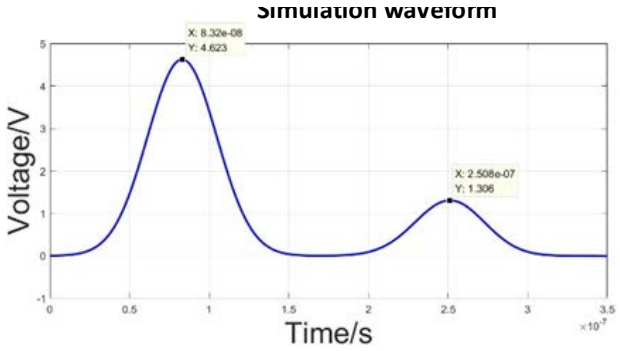

Figure 8 – Simulation waveform.

According to the set RLC and length parameters, in this model, the wave speed is 240μs/m, and an open-circuit fault occurs at 20m. According to the measurement results shown in the figure, D_t =167.6ns, get the distance of fault point D_l =20.11m, the error is 0.6%, in line with expectations.

Then the initial waveform and echo are decomposed by FFT, and their time-domain variation and spectrum are as follows:

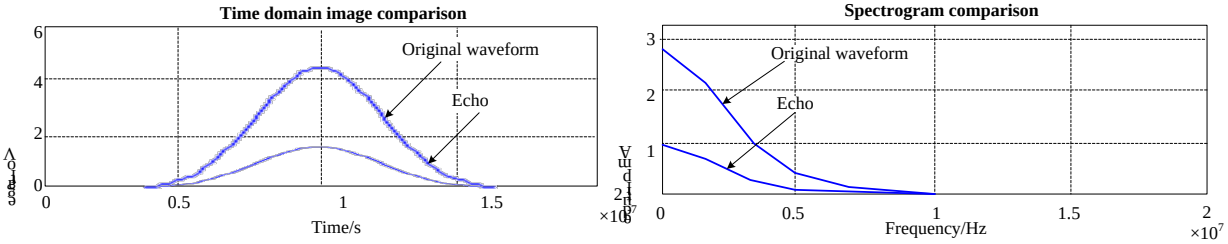

Figure 9 – Time domain and frequency domain images of the transmitted wave and echo of the simulation model.

The simulation results show that the ratio of amplitude attenuation and spectrum attenuation of echo increases from the center to both sides. It is proved that in general, the attenuation constant α does increase with the increase of frequency, and the echo attenuation is consistent with figure 5.

4. Testing and verification

Based on the design idea of the model, a Gaussian pulse generation circuit with adjustable amplitude is built. The overall framework of the hardware part is shown in figure 10. The pulse generator excites the cable to generate echo, and the computer processes the oscilloscope waveform in real time through the set recognition algorithm.

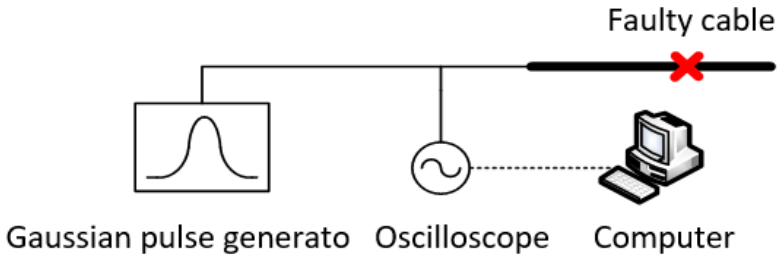

Figure 10 – Test schematic.

Before filtering by oscilloscope, the generated excitation pulse is fitted with the standard Gaussian pulse function, as shown in Figure 11. For the fitting results, the RMSE value is 0.1885 and $R_{\text{-square}}$ is 0.9784, so the oscilloscope filtering can be regarded as Gaussian wave.

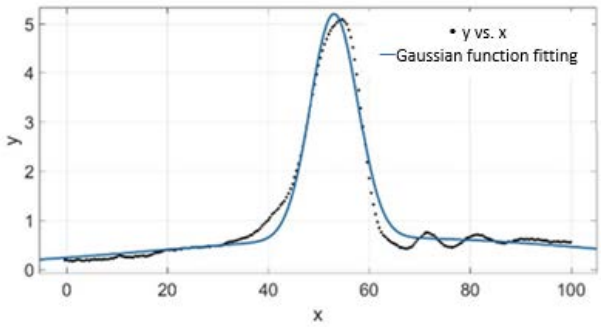

Figure 11 – Fitting of incident wave and Gaussian wave generated by circuit.

In the actual test, the shielded cable with the same specification as the aviation cable used in production and the length of 5 ~ 50m is adopted.

Finally, it is found that the same length of cable (the wave velocity of the actual cable is 254m/us is very stable after five tests. After averaging the five groups of results, the following results are obtained, and the relative error is controlled within 2%.

Table 1 – Experimental results of fault location for different line lengths.

Actual line length(m)	Time interval(ns)	Measuring line length (m)	Absolute error(m)	Relative error
5	40.0	5.08	0.08	1.6%
10	79.5	10.10	0.10	1.0%
15	119.0	15.11	0.11	0.8%
20	157.0	19.94	0.06	0.3%
25	196.5	24.96	0.04	0.2%
30	234.0	29.72	0.28	0.9%
35	275.0	34.93	0.08	0.2%
40	314.6	39.95	0.05	0.1%
45	353.5	44.89	0.11	0.2%
50	393.5	49.97	0.03	0.1%

Then, the following steps are used to realize the detection of cable bandwidth characteristics:

- Use high-speed data acquisition and record the voltage data of the emission waveform to form a data column V_0, and find the peak voltage A_0 by comparing;
- Use high-speed data acquisition and record the reflected voltage data to form a data column V_0, and find out its waveform peak voltage $A_0^{'}$;
- Calculate the scale factor $K=A_0/A_1^{'}$, and multiply all the reflected voltage data by a multiple of K to form a data column $V_0^{''}$;
- Calculate the amplitude difference ratio $\gamma=(V_0-V_0'')/V_0$, when $\gamma>29.3\%$ (attenuation 3dB) appears for the first time, corresponding to the time domain D_x and D_t ;
- From the similarity of the time domain waveform and the frequency domain waveform, according to the position of the sampling point in the entire time domain $D_t = N_xT_s$, the cutoff

frequency of the wire $f_c = f_s/2\pi N_x$.

In the actual test, a certain length of cable is used, with the following waveforms

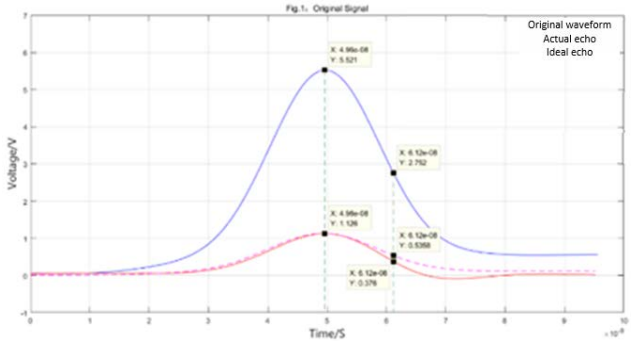

Figure 12 – Experimental results of bandwidth characteristics.

Taking Figure 12 corresponding to a length of 10m as an example, the amplitude attenuation of the echo at 61.2ns is 3dB more than that of the ideal attenuation waveform. This point is the N=30 sampling point from the peak at the sampling frequency of f_s=2.5GHz, so it is converted into the frequency f_c=13.26MHz.

Similarly, it is important to analyze the echo waveforms with different line lengths：

Table 2 – Bandwidth test results of different line lengths

Line length(m)	Sampling frequency(GHz)	Amplitude attenuation point location	Cut-off frequency(MHz)
5	2.5	31	12.84
10	2.5	30	13.26
15	2.5	32	12.43
20	2.5	33	12.06
25	2.5	32	12.43
30	2.5	31	12.84
35	2.5	29	13.72
40	2.5	28	14.21
45	2.5	30	13.26
50	2.5	29	13.72

That is, the bandwidth of this kind of cable is about 13MHz, which is in line with general technical standards.

5. Conclusion

Through theoretical analysis, simulation modeling and actual testing, this paper expounds the application of TDR technology with low-voltage Gaussian pulse as excitation source in the automated test of aviation cables, which has the advantages of simplicity, accuracy and stability.

The subsequent series of experimental results are in line with expectations, and the overall error location of the fault is less than 2%, which proves that this method is indeed an effective aviation cable fault detection method. While realizing the fault location, using the characteristics of the Gaussian wave, the frequency domain is transformed into the time domain, which provides a new idea for bandwidth testing and is innovative.

References

[1] Yongxing, W., et al. Simulation of arcing fault in aircraft wiring system. 2011: IEEE.

[2] Schmidt, M., Practical testing of aircraft wiring and insulation faults. 2002.

[3] Zhang, J.G., et al., Wiring fault detection with Boolean-chaos time-domain reflectometry. Nonlinear

Dynamics, 2015. 80(1-2): p. 553-559

[4] Song, E., et al., Detection and Location of Multiple Wiring Faults via Time–Frequency-Domain Reflectometry. IEEE Transactions on Electromagnetic Compatibility, 2009. 51(1): p. 131-138.

[5] N. G. Paulter. An Assessment on the Accuracy of Time-Domain Reflectometry for Measuring the Characteristic Impedance of Transmission Lines.

[6] Sharma, C.R., C. Furse and R.R. Harrison, Low-Power STDR CMOS Sensor for Locating Faults in Aging Aircraft Wiring. IEEE Sensors Journal, 2007. 7(1): p. 43-50.

[7] Zhang, J., Y. Zhang and Y. Guan, Analysis of Time-Domain Reflectometry Combined With Wavelet Transform for Fault Detection in Aircraft Shielded Cables. IEEE Sensors Journal, 2016. 16(11): p. 4579-4586.

[8] Askari, G. and M. Kamarei, TDR Discontinuity Study Using Gaussian Modulated Ultra Short Pulse in UWB Microwave/mm-Wave Circuits. IEEE Microwave and Wireless Components Letters, 2018. 28(3): p. 260-262.

[9] Kafal M , Cozza A , Pichon L . An efficient technique based on DORT method to locate multiple soft faults in wiring networks. IEEE Autotestcon. IEEE, 2016.

[10] Shi, Q. and O. Kanoun. A novel method for wire fault location using reflectometry and iterative deconvolution. 2012: IEEE.

[11] Bouchekara, H.R.E.H., M.K. Smail and G. Dahman, Diagnosis of Multi-Fault Wiring Network Using Time-Domain Reflectometry and Electromagnetism-Like Mechanism. Electromagnetics, 2013. 33(2): p. 131-143.

[12] Gavita Mugala, Roland Eriksson. Dependence of XLPE Insulated Power Cable Wave Propagation Characteristics on Design Parameters. IEEE Transactions on Dielectrics and Electrical Insulation, 2007. 14(2):p. 393-399.

[13]ith J, Jones B and Brown J. The title of the journal paper. Journal Name, Vol. 1, No. 1, pp 1-11, 2001.

Copyright Statement

The authors confirm that they, and/or their company or organization, hold copyright on all of the original material included in this paper. The authors also confirm that they have obtained permission, from the copyright holder of any third party material included in this paper, to publish it as part of their paper. The authors confirm that they give permission, or have obtained permission from the copyright holder of this paper, for the publication and distribution of this paper as part of the ICAS proceedings or as individual off-prints from the proceedings.